Atmospheric Correction for Case 2 Waters with a Bio-Optical Reflectance Model

J.Vepsäläinen [a,*], J.Pulliainen [b], K. Kallio [a], T.Pyhälahti [a], S. Koponen [b], A. Lindfors [c], K. Rasmus S [d]

[a]Finnish Environment Institute, P.O .Box 140, 00251 Helsinki, Finland -(jenni.vepsalainen, kari.k.kallio, timo.pyhalahti)@environment.fi

[b] Laboratory of Space Technology, Helsinki University of Technology, P.O.BOX 3000, FIN 02015 HUT (jouni.pulliainen, sampsa.koponen)@hut.fi

[c] Luode Consulting, Hietalahdenkatu 7 A 13, FIN-00180 Helsinki, Finland

[d] Division of Geophysics, University of Helsinki, PL 64, 00014 University of Helsinki, FINLAND

Abstract – Two field campaigns were used to demonstrate the usefulness of an atmospheric correction method specifically developed for Case 2 waters. The correction method utilizes bio-optical reflectance modeling and principal component analysis. The MODTRAN radiative transfer code simulations were conducted to obtain a statistical database for varying atmospheric situations. Bio-optical reflectance model takes into account the water quality and it's influence on the detected reflectance. Both field campaigns represent high concentrations of optically active substances such as chlorophyll-a, total suspended sediment and humus. The first field campaign was held at a coastal site of Finland, on the Gulf of Finland, while the other field campaign represents a Finnish lake water area. On both campaigns MERIS satellite instrument and airborne spectrometer data were available.

Keywords: remote sensing, atmospheric correction, bio-optical modelling, water quality, chlorophyll-a

1. INTRODUCTION

In many water quality applications, inadequate atmospheric correction is the main reason for erroneous results in water quality estimation. This is especially the case for the turbid and humic coastal areas, which compound only a small portion of the water bodies. Nevertheless, these water areas, such as the North Sea, coastal areas of Northern America and the Baltic Sea, are important for people for recreational as well as commercial use. Thus, there is a need for developing new and reliable water quality information for these areas.

Combining bio-optical model to atmospheric correction procedure ensures that the optical characteristics of the water region are well representative for the water region under study. A similar approach to ours has been proposed earlier in Land and Haigh, (1996), who present an iterative fitting algorithm for atmospheric correction over Case 2 waters. In our study, for example chlorophyll-a varies from 2 μg/l to 150 μg/l. This has a strong influence on the radiance detected by the satellite or airborne instrument. Other parameters, which affect on the detected signal are the total suspended sediments (TSS) and the amount of CDOM (colored dissolved organic matter). By taking these optically active substances (OAS) into account in the atmospheric correction procedure, reliable estimates of the Top-Of-Atmosphere (TOA) reflectance can be modeled. First, a reliable estimate of the reflectance detected by satellite instrument must be achieved via modeling. Then, the atmospheric correction can be done by inverting the model and calculating the water leaving reflectance from the TOA reflectance.

2. FIELD CAMPAIGN

2.1 Study areas

The first field campaign was held at the Gulf of Finland on the 27th of April, 2004. The Gulf of Finland is the easternmost part of the Baltic Sea, which locates in the Northern Europe. Baltic Sea is a semi-enclosed, humic and has a wide spatial variation in optically active substances. As many turbid water areas, the Gulf of Finland also have a strong seasonal variation in for example chl-a as well as TSS and CDOM. The other field campaign was held at the lake Lohjanjärvi, which is located in the Southern Finland. The lake Lohjanjärvi can be defined as a meso-eutrophic lake. The lake Lohjanjärvi field campaign was held on 5th of August 2004. During the coastal Vuosaari field campaign, a phytoplankton spring bloom dominated the test site, thus giving an exceptional opportunity to test the atmospheric correction in extreme circumstances. The beginning of the transect located near the coast of Helsinki, in the vicinity of a harbour construction place at Vuosaari. The transect continued to the open sea, where the spring bloom was not as intensive as near the coast. Koponen et al. (2004) and Pyhälahti et al. (2004a) describe the Vuosaari field campaign and the measurements in detail.

On both field campaigns, the ground truth data consists of flow through measurements as well as ten water samples collected along a 28 km long transect. The measurement system consist of an AC-9 which measures absorption and scattering coefficients at nine wavelengths between 412 and 715 nm. The measurements are taken from a depth of 0.5 m, which can be considered as a valuable ground truth data for satellite measurements. Altogether, 5103 and 6187 data points were collected with the flow-through system from the Vuosaari and the lake Lohjanjärvi field campaigns, respectively. In addition, on both campaigns, ten water samples were collected along the transect, also from a measurement depth of 0.5 m. Fig. 1 shows the histograms of measured flow-through data on both campaigns as well as the water samples for chl-a, TSS and absorption of CDOM, a_{cdom}. The field measurements were take during 7.30 – 8.45 UTC, which corresponds to local time from 9.30 to 12.45.

2.2 Satellite and airborne data

On both field campaigns, MERIS (The MEdium Resolution Imaging Spectrometer) data was available at the time of field sampling. Airborne campaign was held using airborne spectrometer AISA (Airborne Imaging Spectrometer for Applications). On the Vuosaari coastal site, the flight campaign consisted of four lines at the flight altitude of 1km and one flight line at the flight altitude of 2 km. The flight lines compound a continuous 28 km long transect from the coast to the open sea (Koponen et al. 2004a). The flight campaign at the lake Lohjanjärvi was held using only flight altitude of 2km with seven flight lines. The flight lines at the lake Lohjanjärvi compound a comprehensive image mosaic of the eastern part of the Lake Lohjanjärvi. AISA is a programmable spectrometer i.e. the channel combination can be determined separately for each flight campaigns using wavelengths from 400nm to 900nm. Although it contains 289 channels in total, a reduced amount of channels must be used if an imaging mode is used. On the field campaigns used in this study, AISA spectrometer measured with 32 bands. The bands were selected using the wavelengths measured by MERIS and MODIS instrument. AISA data was geo-coded using a data collected by a GPS-receiver during the flight (Koponen at al 2004a, Pyhälahti et al. 2004).

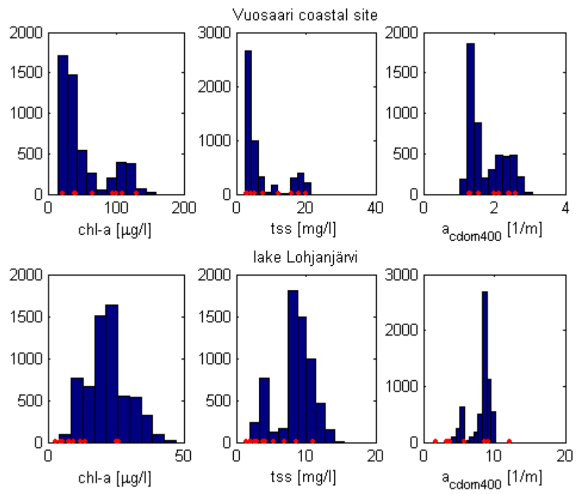

Figure 1. Histograms of chl-a, TSS and $a_{cdom400}$ measured by the flow-through system on both flight campaigns at Vuosaari and at lake Lohjanjärvi. Red dots represent the measured values for OAS's at the sample points. Note that the scale is different for each subplot.

MERIS data were collected from the sample point location and flow-through data locations. The flow-through data points were collected from the distance of a half pixel from the pixel center coordinate (circle radius of 150 m). On average, 30 flow-though measurements were observed within one MERIS pixel. To evaluate the homogeneity of each MERIS pixel, standard deviation of FT data on each MERIS pixel was calculated. Median values for the pixels' standard deviation for chl-a, TSS and $a_{cdom400}$ were 1.38 μg/l, 0.11 mg/l) and 0.07 1/m, respectively. Generally, the standard deviations of chl-a were larger than other optical properties as chl-a varied more within small spatial scale. In this paper, we use the mean value for the OAS's within each MERIS pixel.

3. METHOD

3.1 Bio-optical reflectance model

Atmospheric correction utilizes the bio-optical model to describe the reflectance above the water surface. The bio-optical reflectance model is based on the basic equations presented earlier by Gordon et al (1975) and (1988). This bio-optical reflectance model has been developed for Finnish lakes and is presented in detail in Kallio et al. (2005). Thus, the equations are described here only briefly. ρ^+, which describes the radiance reflectance (or remote sensing reflectance) above water, is defined as a function of simulated underwater irradiance reflectance ρ_- :

$$\rho^+(\lambda) = \frac{s}{Q} * \rho^-(\lambda) + \rho_s \qquad (1)$$

where s is the radiance reduction factor, Q describes the bi-directional character of the upward radiant field and ρ_s is the surface reflectance. The simulated underwater irradiance reflectance $\rho^-(\lambda)$ is determined according to Gordon et al. (1988) as :

$$\rho^-(\lambda) = f * \frac{b_{b,tot}(\lambda)}{[a_{tot}(\lambda) + b_{b,tot}(\lambda)]} \qquad (2)$$

where $b_{b,tot}$ is the total backscattering coefficient, a_{tot} is the total absorption and f is the factor relating the inherent optical properties, $b_{b,tot}$ and a_{tot} to the apparent optical property, the underwater reflectance ρ^-. Total absorption, a_{tot}, is a sum of absorptions by different water constituents i.e. absortions by pure water, cdom, phytoplankton and tripton (Kallio et al., 2005). The other optical property describing the underwater reflectance, the total backscattering coefficient, $b_{b,tot}$, is based on backscattering by pure water and total suspeded sediments according to Kallio et al. (2005).

3.2 Atmospheric correction

The bio-optical model describes the water leaving radiance reflectance ρ^+, based on the equations 1 and 2 and on the measured OAS chl-a, tss and $a_{cdom400}$. The satellite or airborne instrument detects the Top-Of Atmosphere reflectance, ρ_{TOA}. The following equation describes the relationship between the bio-optically modeled radiance reflectance above the water ρ+ and modeled ρ_{TOA}' using the radiative transfer equations:

$$\rho_{TOA}(\lambda)' = \rho_+(\lambda) * \left(\tau_i(\theta_i,\lambda) * \tau_s(\theta_s,\lambda)\right) + \rho_{atm}(\theta_i,\theta_s,\lambda) \qquad (3)$$

In the equation, the $\tau_i(\theta_i,\lambda)$ and $\tau_s(\theta_s,\lambda)$ define the transmission from the sun angle direction and the transmission to the satellite instrument direction, respectively. $\rho_a(\theta_i,\theta_s,\lambda)$ is the atmospheric reflectance to the satellite instrument direction. The atmospheric correction models ρ_{TOA}' via ρ^+ using basic equations of radiative transfer in the atmosphere. The modeled ρ_{TOA}' is then compared with the observed ρ_{TOA}. The atmospheric influence to the detected reflectance is solved by minimizing the difference between the modeled ρ_{TOA}' and satellite observed ρ_{TOA} at each wavelength. At the same time, also the observed OAS's can vary to give better result for the atmospheric correction. This is done by minimizing equation

$$\sum_{1}^{n} \frac{1}{2std(\lambda_i)^2}(\rho_{TOA}(\lambda_i)' - \rho_{TOA}(\lambda_i))^2 + \frac{1}{2std(chl)^2} * (chl' - chl)^2 + \frac{1}{2std(a_{CDOM})^2} * (a_{CDOM}' - a_{CDOM})^2 + \frac{1}{2std(TSS)^2} * (TSS' - TSS)^2 \qquad (3)$$

where chl', TSS' and a_{CDOM}' are the new estimates for chl-a, TSS and a_{CDOM}. The principal idea of this iterative atmospheric correction method has been described earlier in Pulliainen et al. (2001). It has been used earlier also in Koponen et al. (2004b). In the earlier version, only the reflectance information was utilized, thus the water quality estimation was not included in the equation 3. The first iteration assumes that during the time of satellite measurement, the atmosphere is at an average state and the water quality parameters are exactly the field measured values. The atmospheric average state is described using an average transmissivity $<\tau(\lambda_n)>$ and an average atmospheric reflectance $<\rho_{atm}(\lambda_n)>$. To determine the actual state of the atmosphere at time of the satellite observation, an atmospheric parameter γ and principal components of the atmospheric dataset are used. These parameters describe the deviation (γ) from the average atmospheric situation. The first principals of the transmissivity, $\tau_{PCA1}(\lambda)$, and reflectance, $\rho_{a,PCA1}(\lambda)$, are added to the mean reflectance $<\rho(\lambda)>$ and transmissivity $<\tau(\lambda)>$, weighted by the parameter γ. For each wavelength λ, this can be done simultaneously using equation for transmissivity

$$\begin{bmatrix}\tau_{tot}(\lambda)\\ \rho_{atm}(\lambda\end{bmatrix}=\begin{bmatrix}\langle\tau_{tot}(\lambda)\rangle\\ \langle\rho_{atm}(\lambda)\rangle\end{bmatrix}+\gamma\cdot\begin{bmatrix}\tau_{PCA1}(\lambda)\\ \rho_{PCA1}(\lambda)\end{bmatrix} \tag{4}$$

After solving the value for γ by minimizing the equation 3, the atmospherically corrected water leaving reflectance ρ_+' is defined as:

$$\rho_{+'}(\lambda)=\frac{(\rho_{TOA}(\lambda)-\rho_{atm}(\theta_i,\theta_s,\lambda))}{(\tau_i(\theta_i,\lambda)*\tau_s(\theta_s,\lambda))} \tag{5}$$

The $\tau_i(\theta_i,\lambda)$ and $\tau_s(\theta_s,\lambda)$ define the transmission from the sun angle direction and the transmission to the satellite instrument direction, respectively. The product of these equalts to τ_{tot}. $\rho_a(\theta_i,\theta_s,\lambda)$ is the atmospheric reflectance to the satellite instrument direction. The values of the transmissivities $\tau_i(\theta_i,\lambda)$ and $\tau_s(\theta_s,\lambda)$ as well as the atmospheric reflectance $\rho_a(\theta_i,\theta_s,\lambda)$ are defined using the equations 3-4. The pre-calculated atmospheric dataset, which is used in equations 3-5, is calculated with MODTRAN radiative transfer code using varying atmospheric situations.

4. RESULTS AND DISCUSSION

In this preliminary study, the atmospheric correction is presented for the sample point locations as well as the for the flow through data locations. For an airborne spectrometer (AISA), the atmospheric correction is demonstrated using two flight altitudes, 1km and 2km from the Vuosaari coastal site. Figs. 2 a) – c) present the observed (ρ_{TOA}) reflectances (upper grey lines) for AISA and MERIS, atmospherically corrected reflectances, ρ_+' , (lower grey lines) as well as the results of bio-optical modeling, ρ_+ (lower black lines). The modeled $\rho_{TOA'}$ (upper black lines) are also presented for AISA at 2km and for MERIS in Fig. 2b and Fig. 2c, respectively. Fig. 2b presents the results of the 50 first spectras from the flow-through line (AISA 2km), whereas Fig. 2a and Fig. 2c represent the sample point locations.

Fig. 3a and Fig. 3b present the mean value (τ_m, red dots) and standard deviation (τ_{std}, black circles) of transmissivity for the MODTRAN precalculated dataset. Figs. 3a-b show also the solved mean transmissivity (τ_{ms}, red crosses) and the standard deviations (τ_{stds}, black crosses) for a) Vuosaari and b) lake Lohjanjärvi study areas. In case the atmosphere in the study area is reasonably steady, the transmissivity τ should have a small variation around its mean value, contributing to the variations in the atmosphere. As can be seen from the results in Fig. 3b the variation in the atmospheric parameters is small in the lake Lohjanjärvi study area. In contrast to that, there is a clear variation in the solved transmissivity values for the Vuosaari dataset in Fig. 3a. In the results for the Vuosaari study area, the transmissivity increases as the transect goes to the open sea. Near the coast, the transmissivity is smaller. During the measurement campaign, the coast was cloudy and thus influenced on the transmissivity, although the study area was mostly cloud free.

Fig. 4 presents the modeled ρ_{TOA}' values against the observed ρ_{TOA} at the MERIS channels 3-9. The mean wavelengths of MERIS channels 3-9 are shown in the Fig. 4 with different symbols.

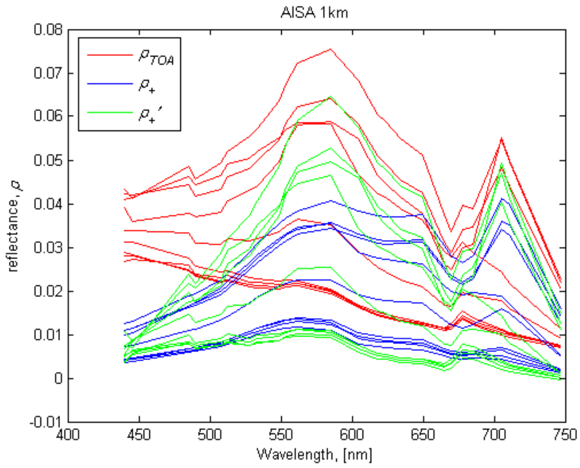

Figure 2a.

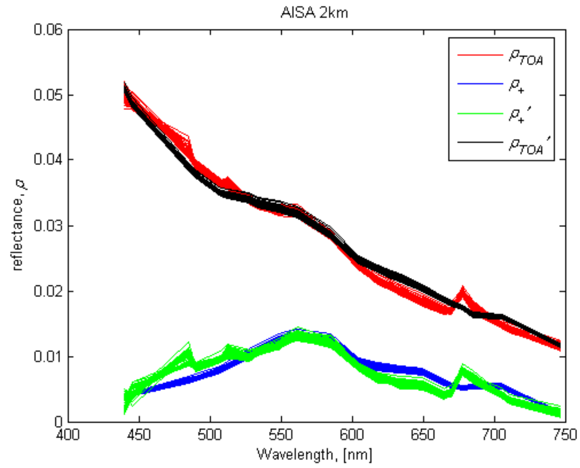

Figure 2b.

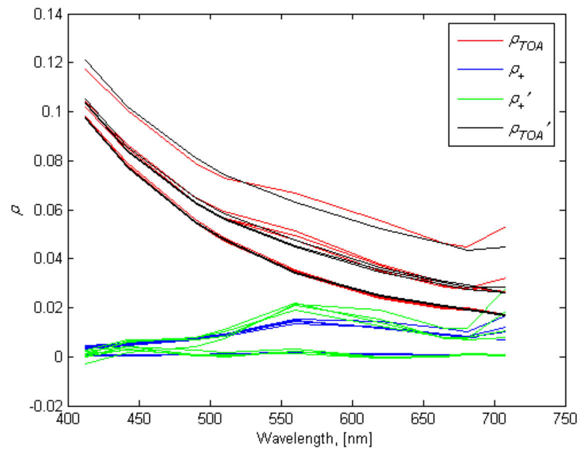

Figure 2c.

Figure 2. Observed (red line, ρ_{TOA}) and atmospherically corrected (green line, ρ_+') as well as modeled (blue line, ρ_+) reflectances for a) AISA at the flight altitude of 1km, b) AISA at 2km, and c) MERIS instrument. In b) and c), also the modeled TOA reflectance, $\rho_{TOA'}$ (black line) is presented.

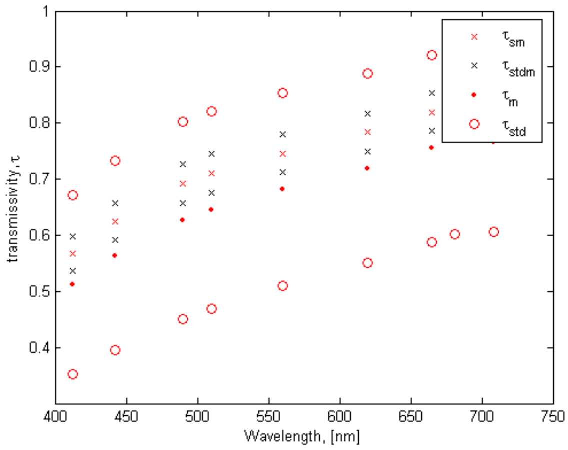

Figure 3a.

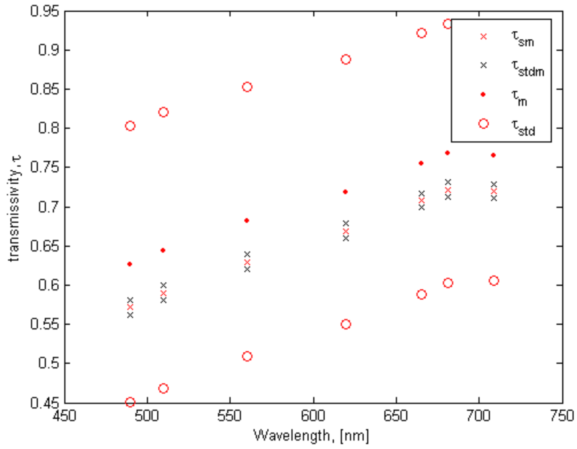

Figure 3b.

Figure 3. Solved mean transmissivities (τ_{ms}, red crosses) and standard deviations for the transmissivities (τ_{stds}, black crosses) for a) Vuosaari and b) lake Lohjanjärvi flow-through dataset. Red dots are the mean transmissivities (τ_{m},) and red circles are standard deviations (τ_{std},) for the whole precalculated MODTRAN dataset. Mean transmissivity in MODTRAN dataset represents an average state of atmosphere $<\tau_{tot}>$ in equation 4.

5. CONCLUSIONS

This paper presented an iterative method for atmospheric correction at Case 2 waters. The principal idea is to combine bio-optical model to atmospheric correction procedure and thus retrieve more reliable results for the water quality estimation via remote sensing. The preliminary results were presented for MERIS satellite instrument data as well as for airborne spectrometer AISA at two flight altitudes, 1km and 2km. The results show that the method is usable for an atmospheric correction in the Case 2 waters, although it needs further improvements for operational use. At the moment, the method can be applied for individual points. The method is able to correct the atmospheric influences in the spectral data with sufficient accuracy.

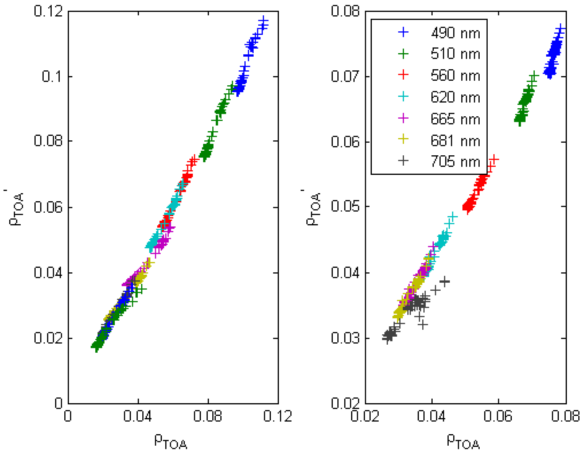

Figure 4. Modelled ρ_{TOA}' plotted against MERIS observed ρ_{TOA} for Vuosaari (left) and lake Lohjanjärvi (right) flow-through data points for wavelengths between 490nm and 705nm.

6. REFERENCES

Gordon, H.R., Brown O.B, and Jacobs M. M., Computed relationships between the inherent and apparent optical properties of a flat homogeneous ocean, Applied Optics, 14, 417-427, 1975.

Gordon H.R., Brown, O.B., Evans, R.H., Brown, J.W., Smith, R.C., Baker, K.S., and Clark, D.K., A semianalytical radiance model of ocean color, Journal of Geophysical Research, vol. 93, no. D9, p.p. 10909-10924, 1988.

Kallio, K., Pulliainen, J., and Ylöstalo, P., MERIS, MODIS and ETM+ channel configurations in the estimation of lake water quality from subsurface reflectance using semi-analytical and empirical algorithms, Submitted to Remote Sensing of Environment. 2005.

Koponen S., Pulliainen J., Kallio K., Vepsäläinen J., Pyhälahti T., Lindfors A., Rasmus K.. Coastal Monitoring of Water Quality in the Gulf of Finland Using Airborne and Satellite Instruments together with a Flow-through Measurement System. Ocean Optics XVII, Fremantle, Australia October 2004. 2004a.

Koponen S., Kallio K., Pulliainen J., Vepsäläinen J., Pyhälahti T., Hallikainen M.. Water Quality Classification of Lakes Using 250-m MODIS Data, IEEE Geoscience and remote sensing letters vol 1 no. 4, p.p. 287-291, 2004b.

Koponen S., Pulliainen J., Servomaa H., Zhang Y., Hallikainen M., Kallio K., Vepsäläinen J., Pyhälahti T., Hannonen T.. An analysis on the feasibility of multi-source remote sensing observations for chl-a monitoring, The Science of Total Environment, vol 268, no. 1-3, p.p. 95-106, 2001.

Land and Haigh, (1996), Atmospheric correction over case 2 waters with an iterative fitting algorithm, Applied Optics, vol. 35, no. 27, p.p. 5443-5451.

Pulliainen J., Vepsäläinen J., Kallio K., Koponen S., Pyhälahti T., Härmä P, Hallikainen M.. Monitoring of Water Quality in Lake and Coastal Regions Using Simulated ENVISAT MERIS Data. Proceedings of ESA ERS-ENVISAT Symposium, Göteborg, pp. 10, October, 2000.

Pyhälahti, T., Vepsäläinen, J., Kallio, K., Pulliainen, J., Koponen, S., Lindfors, A., Rasmus, K. Spatial Variability of Coastal Water Quality and Its Influence on Measurements With Low and Medium Resolution Satellite Instruments. Ocean Optics XVII, Fremantle,Australia, October 2004.